Asian Journal of Atmospheric Environment
Vol. 9-1, pp. 1-11, March 2015
doi: http://dx.doi.org/10.5572/ajae.2015.9.1.001

ISSN(Online) 2287-1160
ISSN(Print) 1976-6912

# Evaluation of the Effect of Regional Pollutants and Residual Ozone on Ozone Concentrations in the Morning in the Inland of the Kanto Region

**Yusuke Kiriyama*, Hikari Shimadera[1)], Syuichi Itahashi[2)], Hiroshi Hayami[2)] and Kazuhiko Miura**

Tokyo University of Science, Tokyo, Japan
[1)]Center for Environmental Innovation Design for Sustainability, Osaka University, Osaka, Japan
[2)]Central Research Institute of Electric Power Industry, Abiko, Japan

*Corresponding author. Tel: +81-3-5228-8215, E-mail: j1212703@ed.tus.ac.jp

## ABSTRACT

Increasing ozone concentrations are observed over Japan from year to year. One cause of high ozone concentration in the Kanto region, which includes areas inland from large coastal cities such as metropolitan Tokyo, is the transportation of precursors by sea breezes. However, high ozone concentrations are also observed in the morning, before sea breezes approach inland areas. In this point, there would be a possibility of residual ozone existing above the nocturnal boundary layer affects the ozone concentration in the following morning. In this study, we utilized the Weather Research and Forecasting model and the Community Multiscale Air Quality model to evaluate the effect of regional precursors and residual ozone on ozone concentrations over the inland Kanto region. The results show that precursors emitted from non-metropolitan areas affected inland ozone concentrations more than did precursors from metropolitan areas. Moreover, calculated results indicate downward transportation of residual ozone, resulting in increased concentration. The residual ozone was also affected by precursors emitted from non-metropolitan areas.

**Key words:** Surface ozone, WRF, CMAQ, Regional air pollution, Boundary layer

## 1. INTRODUCTION

Photochemical oxidant (or simply ozone) air pollution first occurred in Japan in the 1970s, and was then considered a social issue. Annual mean ozone concentration in Japan has increased since 1980s. Possible causes of high ozone concentration include transboundary air pollution from Asian industrial countries, increased total ozone in the troposphere, settling of stratospheric ozone, and the effect of domestic pollutant sources. Focusing on the Kanto region in Japan (the area in and around metropolitan Tokyo on the Pacific coast of Japan) during summer, seasonal wind from the Pacific Ocean dominates wind patterns and blocks air masses approaching from inland. Pochanart *et al*. (2002) showed reduced inland air mass to the Pacific coast of Japan in summer relative to other seasons by monitoring pollutants at remote islands and performing backward trajectory analyses. Therefore, the effect of transboundary air pollution is relatively smaller than in other seasons. It is well known that amounts of ozone settling from the stratosphere peak for mid-latitudes in springtime (Muramatsu, 1980) and that there is a reduced effect in summertime. Precursor sources in and around the Kanto region will therefore have the greatest effect on ozone concentration in this area during summertime. One factor behind high ozone concentration inland from large coastal cities is the transportation of precursors by sea breezes (e.g. Schade *et al*., 2011). There have been many studies of transportation by sea breeze in the inland Kanto region. For example, Wakamatsu *et al*. (1983) showed typical sea-land breeze transport patterns and vertical distribution of precursors. There are also cases of high ozone concentration in the inland Kanto region before sea breezes approach in the morning (Kiriyama *et al*., 2012). As a result, high ozone concentration is sustained from mid-morning to early evening in the region. Long exposure to high ozone concentration is a health and environmental problem. Local emissions are considered a major cause of high ozone levels, but no detailed evaluation of morning high ozone concentration has been conducted in the inland Kanto region. It therefore remains unclear whether precursors emitted from the inland Kanto region, which are relatively less than those generated in the metropolitan area, can result in ozone concentrations nearly equal to those of the metropoli-

tan area alone (Hosoi *et al*., 2012). The contribution of precursors emitted from the metropolitan area and that of inland areas remains unknown. If ozone exists above the nocturnal layer containing the low concentration NOx, ozone is in a better position to stay over night on the layer because NO and ozone is difficult to react. This ozone residual layer forming above the nocturnal boundary layer was reported by Niwano *et al*. (2007) and Lin *et al*. (2010), the latter of which showed that downward transport of residual ozone can affect morning ground-level ozone concentration. In the Kanto region, however, there have been no evaluations of the extent to which residual ozone is involved in morning surface ozone concentrations, or of the contribution by precursors from metropolitan and other areas.

The present study uses a meteorological model and a chemical transport model to evaluate the effect of regional precursors and residual ozone on ozone concentrations, especially in the morning inland of the Kanto region during the summer season.

## 2. METHODS

For air quality simulations, we used the Weather Research and Forecasting (WRF) model version 3.2.1 (Skamarock *et al*., 2008) and the Community Multiscale Air Quality (CMAQ) model version 4.7.1 (Byun and Schere, 2006). The calculation period was 16 July to 8 August 2010, with the first 4 days used as a spin-up period. The results and discussions below therefore use the results from 20 July to 8 August. During this period, high ozone concentrations were continuously observed in the inland Kanto region. The model consists of three domains from domain 1 (D1), covering a wide area of East Asia, to domain 3 (D3), covering most of the Kanto region (Fig. 1). In the WRF simulation, D1 consist of $109 \times 93$ grids (64 km × 64 km per 1 grid), domain 2 (D2) consist of $73 \times 73$ grids (16 km × 16 km per 1 grid) and D3 consist of $97 \times 97$ grids (4 km × 4 km per 1 grid). As input data to the WRF model, for meteorology we used final analysis data provided by the National Center for Environmental Prediction (NCEP), and meso-analysis data provided by the Japan Meteorological Agency (JMA) (used for D2 and D3), and for sea surface temperature we used real-time global sea surface temperature analysis data provided by NOAA/NCEP. Three-dimensional analysis nudging was applied to the west-east and north-south wind components in D1 and D2, with the nudging coefficient set to $1.0 \times 10^{-4}$ s$^{-1}$ for the entire simulation period. For initial and boundary conditions of the CMAQ calculation, we used the results calculated by MOZART4/GEOS5 (Emmons *et al*., 2010) for D1, and simulated results for the outer domains D2 and D3. WRF/CMAQ was configured with the same physics and chemistry options as those used by Shimadera *et al*. (2013). The emission data for the base case simulation except for volcano emission were produced from the dataset described by Shimadera *et al*. (2014).

In addition to the base simulation, in D3 we conducted emission-controlled simulations and simulations with no chemical reaction. As Fig. 1 shows, we divided the Kanto region into two areas. One is the interior of the circle, defined by reference to Route 16, with radius about 40 km centered on central Tokyo (labeled "metropolitan" in Fig. 1). The other area is the exterior of this area (labeled "non-metropolitan" in Fig. 1). In this study, metropolitan cases indicate no emissions in the metropolitan area, and non-metropo-

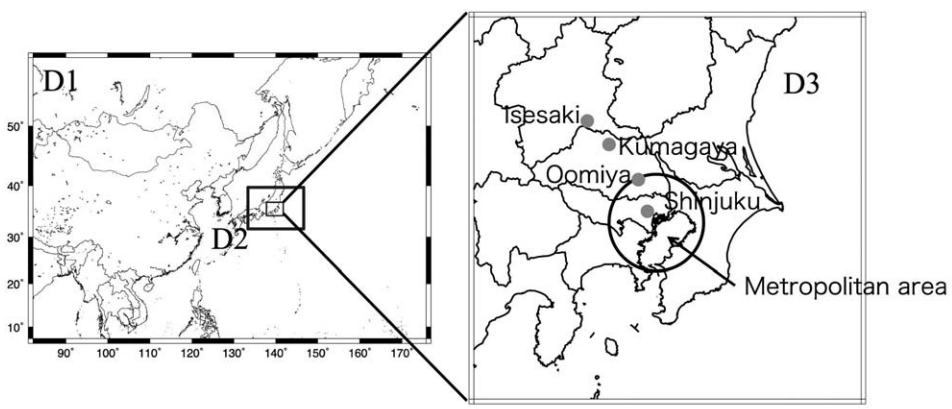


**Fig. 1.** Horizontal model domain used for CMAQ. The black circle divides the Kanto region into two areas, a metropolitan area (inside area of the circle) and a non-metropolitan area (outside area of the circle). Black circle was defined by reference to Route16. Gray points indicate locations of diagnostic points in the Kanto region: Isesaki, Kumagaya, Oomiya, and Shinjuku.

**Table 1.** Total amount of precursors emitted from D3, and amounts of precursors emitted from metropolitan area and non-metropolitan area.

| Emission area | NOx Amounts (g/25 days) | VOCs Amounts (g/25 days) |
|---|---|---|
| D3-wide | $1.83 \times 10^{10}$ | $8.27 \times 10^{10}$ |
| Metropolitan area | $6.90 \times 10^{9}$ (about 38% of D3-wide) | $1.61 \times 10^{10}$ (about 37% of D3-wide) |
| Non-Metropolitan area | $1.14 \times 10^{10}$ (about 62% of D3-wide) | $6.66 \times 10^{10}$ (about 63% of D3-wide) |

litan cases indicate no emissions in the non-metropolitan area. Table 1 summarizes the amounts of emission from metropolitan and non-metropolitan area and the total amount of emissions in D3. That table shows that precursors emitted from metropolitan area include $6.90 \times 10^9$ g of NOx, and $1.61 \times 10^{10}$ g of VOCs over 25 days, accounting for approximately 40% of total NOx and VOC emissions. Non-metropolitan areas have more precursors than the metropolitan area, but metropolitan areas have far more precursors per unit area. Contributions from each area were calculated as the difference between the base and each emission-controlled case for ozone concentration. We investigated causes of high ozone concentration by evaluating the contribution of each emission area from these differences. If the ozone concentration increases under no chemical reaction condition, the increase will be influenced by horizontally or vertically transported ozone as distinct from in situ generation by photochemical reactions. Moreover, the increase of ozone will be mostly influenced by vertical ozone transport if horizontal ozone distribution is almost uniform and wind speed is slow. Therefore, to evaluate the effect of downward transport of residual ozone for ground-level ozone concentration, we conducted the no chemical reaction (No_chem) simulation. In the no chemical reaction (No_chem) case, the simulation starts at 05:00 Japan Standard Time (JST, UTC+9 hours; times are given as JST below) and uses base simulation results of D3 for initial conditions and no chemical reaction, and the simulation stops at 05:00 the next day, a 24-h cycle. In the No_chem case, $O_3$ concentrations for this case will be shown. In this study, boundary condition which is used in base case applied to all cases. Initial condition of base simulation applied to metropolitan and non-metropolitan cases. In this study, emissions in each emission-controlled case from corresponding ocean area is also zero.

Observed ozone concentration data used in this study were obtained from the Atmospheric Environmental Regional Observation System (AEROS, http://www.nies.go.jp/igreen/, in Japanese). In this study, the high ozone concentration criterion was defined as 120 ppb, in accordance with the standard criterion for photochemical oxidant advisories in Japan.

In this study, the words "Inland areas" are used in the sense of the area in and around Kumagaya and the north.

## 3. RESULTS AND DISCUSSION

### 3. 1 Temporal Change in Ozone Concentration and Reproducibility of Base Simulation Results

Fig. 1 shows the locations of Shinjuku in metropolitan Tokyo, Oomiya in Saitama Prefecture, Kumagaya in Saitama Prefecture, and Isesaki in Gunma Prefecture. These four points are located on the main approach path of sea breezes and are used as representative locations for ozone concentrations. Isesaki and Kumagaya are representative of inland area and Shinjuku and Oomiya are representative of coastal area. Fig. 2 shows a time series of observed and base simulation results at Shinjuku, Oomiya, Kumagaya, and Isesaki. As shown in Fig. 2, two south points and inland points have different diurnal pattern. Observed ozone at two south points have one daily peak and two inland points have two daily peaks, especially in the early days of the study period. Fig. 3 shows the hourly averaged ozone concentration at two inland points. The averaging period is 20 to 24 July, high concentration continuously occurred. As shown in Fig. 3, variation at Kumagaya shows two daily peaks. The first peak appeared at 13:00 and the second peak appeared at 18:00. At Isesaki, Daytime maximum concentration occurred at 15:00 and the second peak appeared at 20:00. In inland area in the high concentration days, ozone concentration can takes two daily peaks. The temporal difference between ozone concentration peaks at Oomiya and Kumagaya is 1 or 2 h, and at Kumagaya and Isesaki is 2 h. This temporal difference is due to sea breeze transport. Comparing the observed and base simulation results, the base simulation at Kumagaya and Oomiya overestimated observed ozone concentrations, especially in the latter half of this period. For nighttime data, the base simulation results of all four points overestimated the observed results, but simulations and observations are in good agreement for daytime temporal variation. At Isesaki, ozone concentration peaks are also well esti-

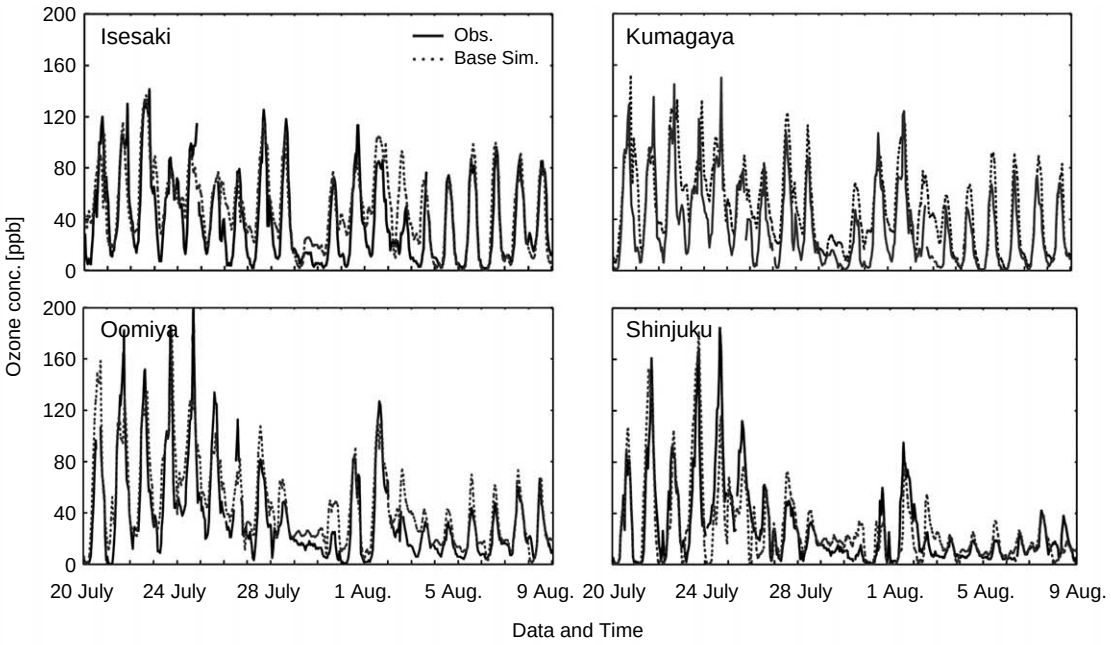


**Fig. 2.** Time series of ozone concentration of observed and base case simulation results at points shown in Fig. 1. Solid lines indicates observed ozone concentrations and dotted lines indicates base case simulation results.

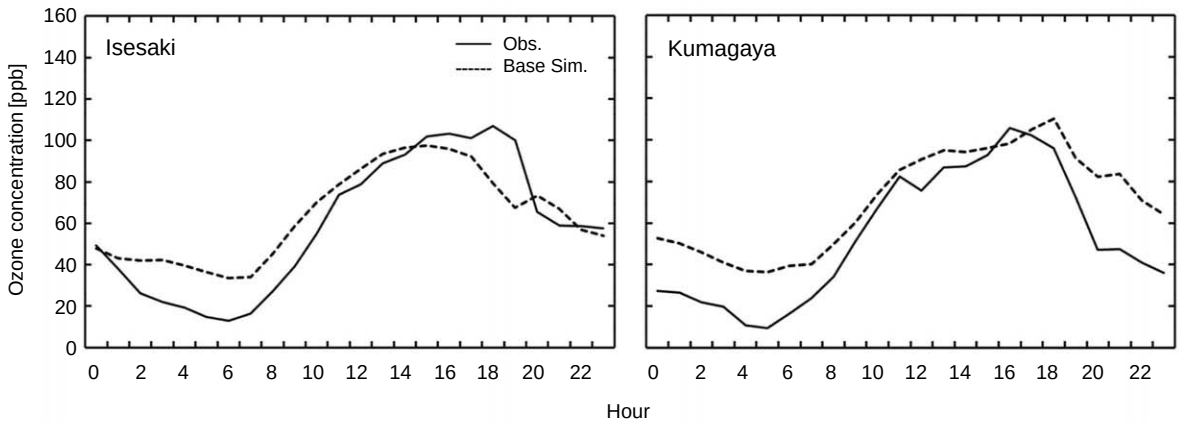


**Fig. 3.** Hourly averaged ozone concentrations at Isesaki and Kumagaya. Averaged period is 20 to 24 July.

mated by the base simulation. The scatter plots in Fig. 4 show that the base simulation correlates well with observations. The base case overestimated more than twofold at the low concentration field, which corresponds to nighttime data. At these four points, ozone concentrations were above 120 ppb for several days of observation and base simulation data. In particular, from 20 to 24 July high ozone concentrations continuously occurred in the inland Kanto region. Ozone concentration was low at Shinjuku and Oomiya from 5 to 8 August, but ozone concentration increased up to about 80 ppb at Kumagaya and Isesaki during this period. This study focuses on high ozone concentration in the inland Kanto region, so we analyzed these two periods.

## 3. 2 Contribution of Emission Areas for the Inland Kanto Region.

### 3. 2. 1 Period from 20 to 24 July

Fig. 5 shows a time series of the base simulation results and the contribution of metropolitan and non-metropolitan areas at Isesaki and Kumagaya from 20 to 24 July. This and the following corresponding fig-

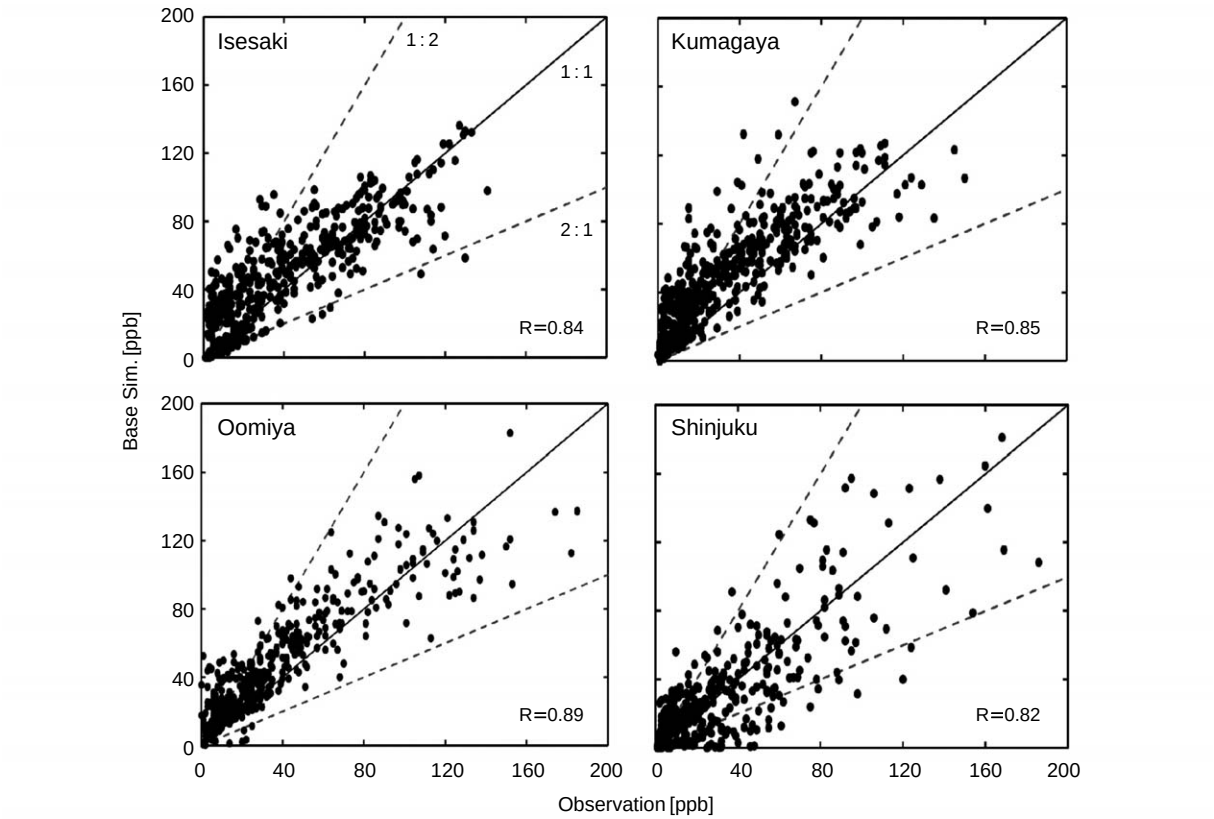


**Fig. 4.** Scatter plots of observed versus simulated ozone concentration for the period from 20 July to 8 August at the points shown in Fig. 1. R shown in each plot is correlation coefficient.

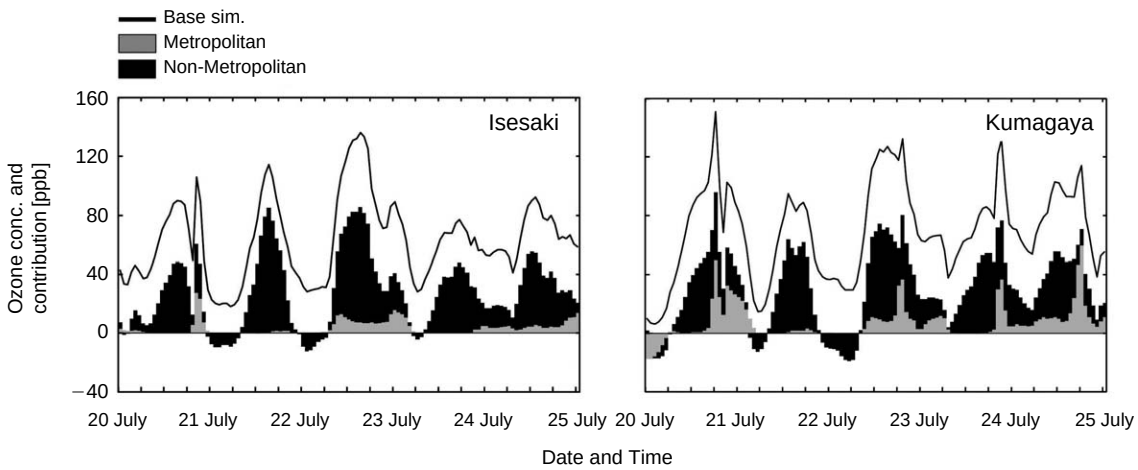


**Fig. 5.** Time series of ozone concentration in the base case simulation and contribution of metropolitan and non-metropolitan areas from 20 to 25 July at Isesaki(left) and Kumagaya(right).

ure show differences between the base simulation results and the sum of contributions. These differences are caused by transport from the outer domain and the nonlinear relationship between ozone concentration and emitted precursors. Around of these two points, 80-100 ppb ozone is generated by 12:00 in several days of this period, during which contribution of the metropolitan area was low, and that of the non-

metropolitan area was the main factor behind high ozone concentration in the morning. After midday, the metropolitan area contribution has increased due to transport of precursors emitted from the coastal area by sea breeze. Focusing on 22 July, when ozone concentration was the highest in this period, the contribution of the non-metropolitan area is 45-70% and that of the metropolitan area is less than 10% in the morning. In other days there are cases where the contribution from the metropolitan area was up to about 50% at Kumagaya, but the metropolitan area had a lower contribution to high ozone concentration at Isesaki.

The additional sensitivity simulations of which set the emission reduction rates to 50% and 20% in metropolitan and non-metropolitan area were also conducted to assess the uncertainty of contribution associated with the reduction rates. In Isesaki and Kumagaya, uncertainty of contribution of metropolitan area was 10% to 20% and non-metropolitan was about 10%.

Fig. 6(a) shows the spatial distribution of ozone concentration predicted by the base simulation for 22 July, and Fig. 6(b) and (c) show the contributions of the metropolitan and non-metropolitan areas for the same day. Fig. 6(a) shows a high ozone concentration of about 90 ppb at 09:00 in parts of the inland Kanto region. The sea breeze did not extend inland by 12:00, but ozone concentrations had reached about 130 ppb at Isesaki and its surrounding. A part of west side of

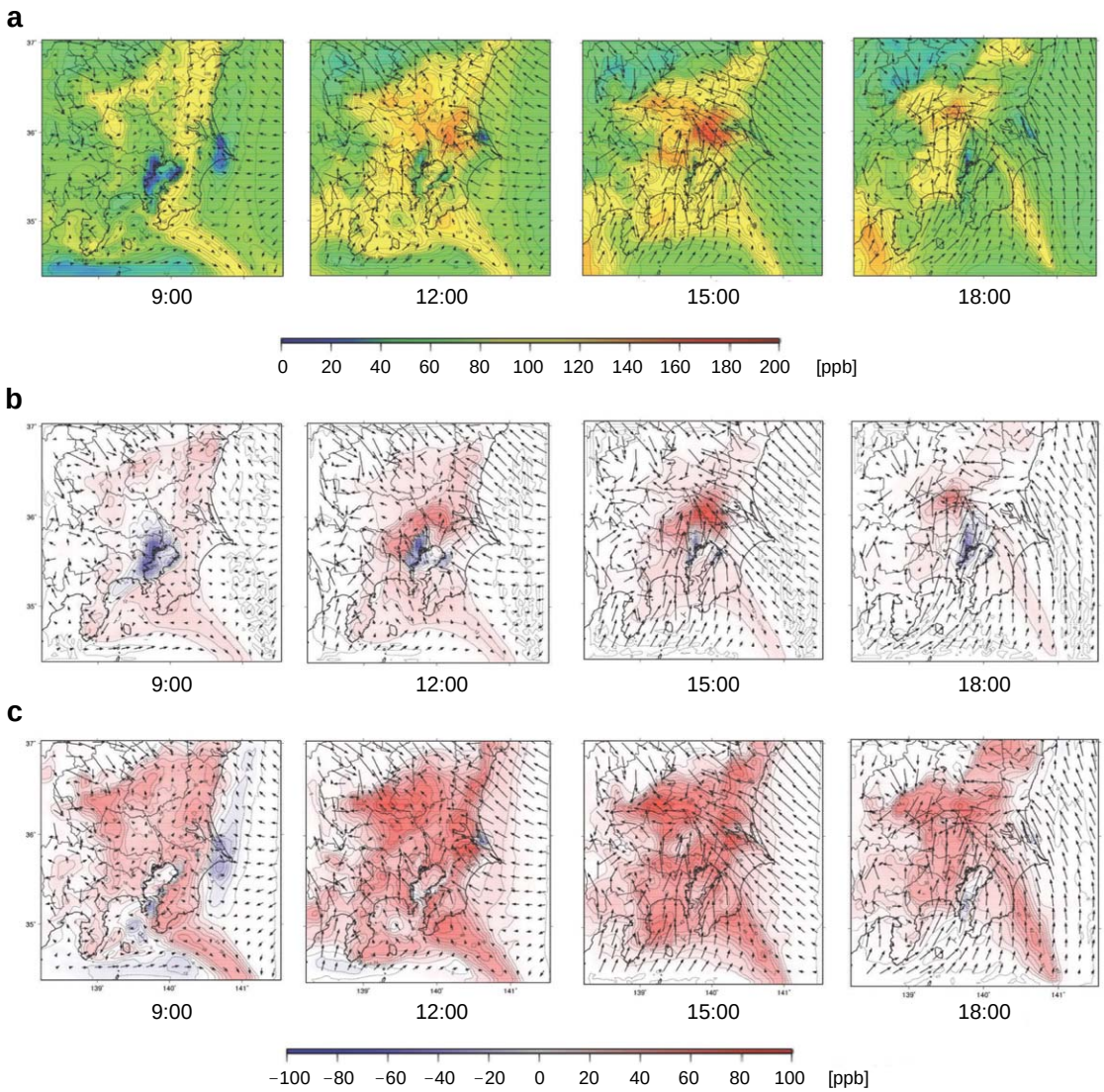


**Fig. 6.** Spatial distribution of (a) ozone concentration and contribution of (b) metropolitan and (c) non-metropolitan areas on 22 July.

Kanto also reached 130 ppb. At 09:00, precursors from the metropolitan area contributed to inhibiting ozone generation in the coastal area. In inland, the contribution of the metropolitan area was low (10% or less). The contribution from non-metropolitan areas was high from 09:00 to 12:00 over almost the entirety of the Kanto region. The distribution of high ozone concentration was in good agreement with the contribution of non-metropolitan areas, especially inland. This finding indicates that, in this period, a major factor for morning high ozone concentrations in the inland Kanto region was precursors emitted from non-metropolitan areas. After midday, sea breezes transport precursors from the coastal area to the inland area, and these precursors affected the ozone concentration. At 15:00, contribution of the metropolitan area became greater than 12:00 on the air mass which sea breeze transporting. Contribution of non-metropolitan area is about 60 to 80 ppb, near level to contribution of metropolitan area on the air mass. After 15:00, the contribution of the metropolitan area decreased over the entire Kanto region, and precursors from non-metropolitan areas were a dominant factor behind the ozone concentration.

### 3. 2. 2 Period from 5 to 8 August

Fig. 7 shows the same as Fig. 5 but from 5 to 8 August. During this period, contributions were often negative due to titration by NOx emitted from each area at nighttime and in the early morning. In the morning, the contribution of the metropolitan area accounted for around 10% at Isesaki and Kumagaya, while the non-metropolitan contribution accounted for 20-67% at Isesaki and 20-50% at Kumagaya. From 20 to 24 July (the period discussed in section 3.2.1), non-metropolitan areas had a higher effect and metropolitan areas had a lower ozone generation effect. Comparing 20 to 24 July and 5 to 8 August at Kumagaya, the ozone concentration was lower from 5 to 8 August than from 20 to 24 July when the contribution is nearly the same value. But at Isesaki, the metropolitan contribution increased compared to 20 to 24 July and affected ozone generation. After midday, the sea breeze arrived at Kumagaya from 13:00 to 14:00 and at Isesaki from 15:00 to 16:00, and the metropolitan contribution increased at these times. Additionally, the metropolitan area had small effect on ozone generation at Isesaki from 20 to 24 July, but during this period contributed about 20 ppb to ozone concentration after sea breeze passage, similar as at Kumagaya.

Fig. 8 shows the same as Fig. 6 but for 6 August. As Fig. 8(a) shows, at 09:00 up to 60 ppb ozone was distributed in some parts of the inland Kanto region. In such relatively high-concentration areas, the metropolitan contribution is several ppb, but the non-metropolitan contribution accounts for about 50% in this area and is a major factor behind ozone concentration in the inland-Kanto region at this time. At 12:00, 70-90 ppb ozone is distributed inland. Wind speed simulated for this area is faster than at 09:00, and winds are southerly. Similar distribution patterns appeared in the ozone concentration and the non-metropolitan contribution in this period, so most highly ozone-polluted areas had a little contribution from the metropolitan area, and were affected by precursors from non-metropolitan areas in the same manner as on 22 July (discussed in section 3.2.1). At 15:00, precursors transported by sea breeze from the coastal area spread around Isesaki and Kumagaya, contributing to ozone. The metropolitan contribution increased in compari-

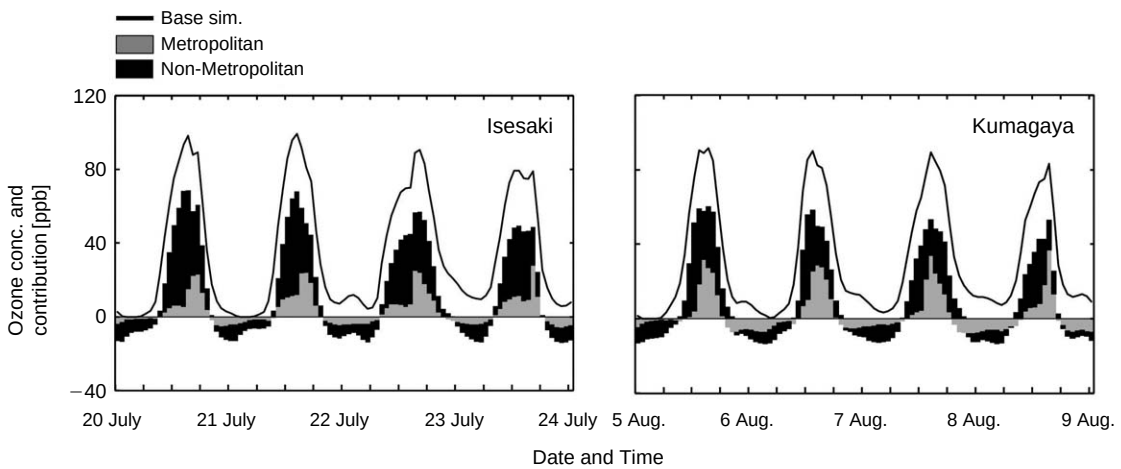


**Fig. 7.** Time series of ozone concentration of the base case simulation and contribution of metropolitan and non-metropolitan areas at Isesaki (left) and Kumagaya (right) from 5 to 8 August.

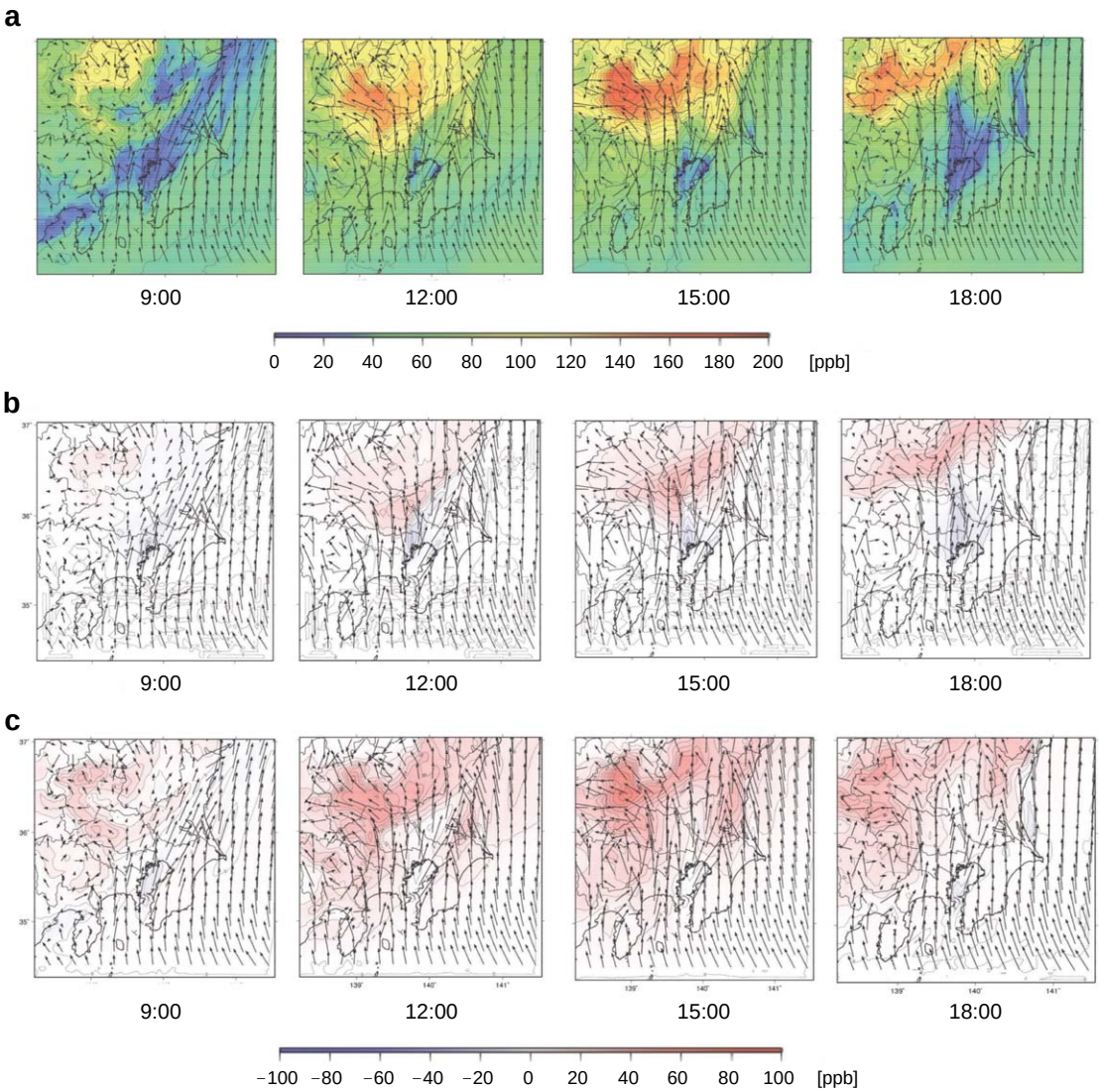


**Fig. 8.** Spatial distribution of (a) ozone concentration and contribution of (b) metropolitan and (c) non-metropolitan areas on 6 August.

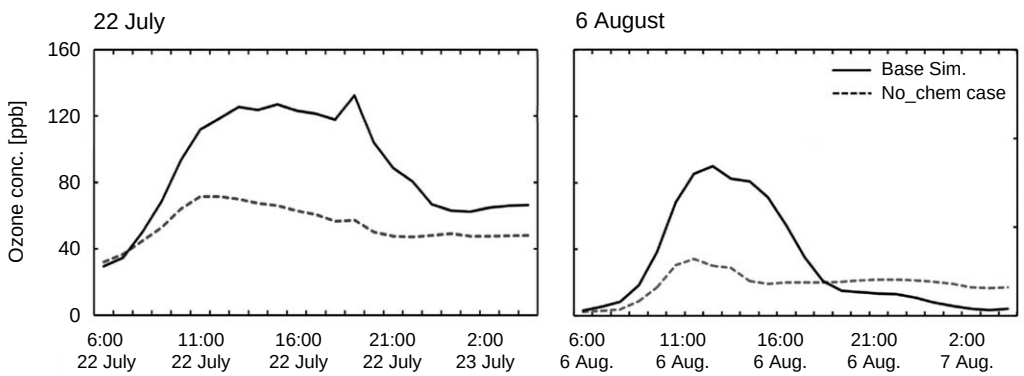


**Fig. 9.** Time series of ozone concentration in the base case and No_chem case simulations at Kumagaya on 22 July and 6 August. Solid lines indicate base case simulation results and broken lines indicates No_chem case simulation results.

son with 22 July, and in some locations exceeded the non-metropolitan contribution, but in many high ozone areas there was a higher non-metropolitan contribution. At 18:00, areas where the effect of the metropolitan area reached similar level as that of the non-metropolitan area extended to remote parts of the Kanto region, and ozone distribution paralleled the contribution of the metropolitan area. The metropolitan area made a larger contribution to ozone concentration in the inland Kanto region than the period from 20 to 24 July, but this contribution did not exceed that of the non-metropolitan area. These findings indicate that during this period, too, precursors from non-metropolitan areas were a major factor behind high ozone concentration.

### 3. 2. 3 Relation of Upper Residual Ozone and Morning Surface Ozone Concentration

Fig. 9(a) and (b) show a time series for results of the base simulation and the No_chem case simulation at Kumagaya on 22 July and 6 August. There are some discontinuous points in the No_chem case resulting from the changing initial conditions and restart calculations that were explained in Section 2. As shown in Fig. 9(a) and (b), ozone concentration increased 20-30 ppb in spite of there being no chemical reaction. Ozone concentration in the No_chem case accounts for 40-80% of the base simulation by 10:00 in days between 20 July and 8 August, when the ozone concentration increased 30 ppb from the minimal morning value. This phenomenon is also seen in other days, especially in the period from 5 to 8 August discussed in the previous section, during which this occurred each morning. Furthermore, this phenomenon occurred not only in Kumagaya but also in Isesaki and other points of inland Kanto region, suggesting that this is not a local phenomenon. The reason for increased ozone concentration in a non-chemical reaction environment is likely horizontal or vertical transport. In Figs. 6 and 8 the inland wind speed was slow, and ozone concentration was distributed uniformly at 09:00. Horizontal transport therefore likely has little effect on ozone concentration, and vertical transport from the upper air to near the surface will be the main factor behind increased ozone.

Fig. 10(a), (b), and (c) show time height cross sections of ozone concentration simulated in the No_chem case, and the metropolitan and non-metropolitan contributions at Kumagaya on 22 July, respectively. Solid lines shown in Fig. 10(a), (b) and (c) indicate the PBL height. As Fig. 10(a) shows, residual ozone of about 80-100 ppb were detected from 550-1100 m from 05:00 to 09:00. Isopleth lines extend downward from 7:00 to 11:00, indicating entrainment of residual ozone near the surface, during which time the surface ozone concentration increased the entrainment. This

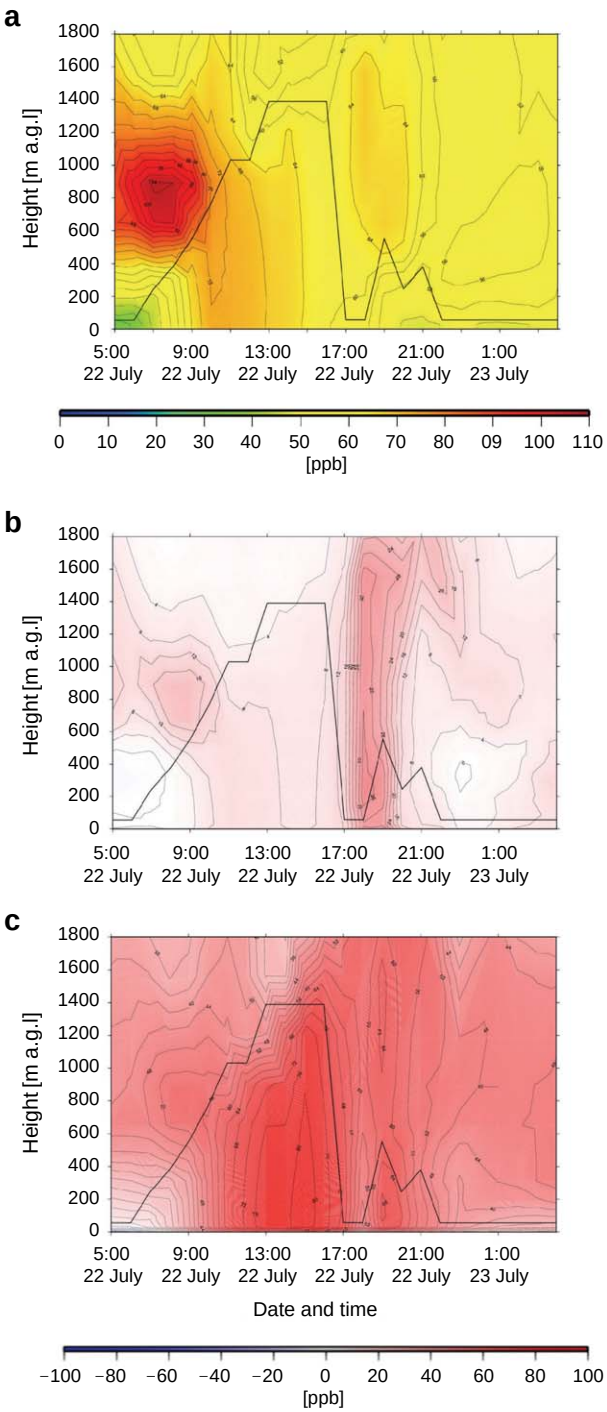


**Fig. 10**. Time-height cross section of (a) No_chem case simulation ozone concentrations and the contribution of (b) metropolitan and (c) non-metropolitan areas at Kumagaya from 5:00 22 to 4:00 23 July. Solid lines indicate the PBL height.

phenomenon indicates that the upper residual ozone will be another factor behind increasing ozone, Increasing the importance of ozone concentrations in the upper air during early morning. In the episodes analyzed in this study, also important is that emission reduction in non-metropolitan area is more effective in this upper air ozone. As shown in Fig. 10(b), there was a relatively high metropolitan contribution in the upper air as compared to near the surface. Yet the contribution of the non-metropolitan area to residual ozone was about 50 ppb, accounting for about 50% of the No_chem case result; the non-metropolitan contribution thus constitutes a large portion of ozone entrained from the upper air.

## 4. CONCLUSIONS

To address the problem of high ozone concentrations, especially during morning, in the inland Kanto region of Japan, we investigated the ozone concentration response to emissions from emissions from metropolitan and non-metropolitan using the WRF model and the CMAQ model. Focusing on 22 July, the metropolitan contribution accounted for less than 10% of the base simulation result. On other high ozone days in the period from 20 to 24 July, the metropolitan contribution was nearly zero in the mornings, and the non-metropolitan contribution accounted for 45-70%. In contrast, during the period from 5 to 8 August, during which relatively high ozone occurred with regularity in Isesaki and Kumagaya, both metropolitan and non-metropolitan contributions appeared throughout the day. But also during this period the non-metropolitan area significantly affected inland ozone concentrations, with contributions of 20-60% at Isesaki and 20-50% at Kumagaya. The spatial distribution also showed that non-metropolitan areas contributed to inland ozone concentrations. The example of 22 July shows that precursors from the metropolitan area had a small, narrow effect inland. The example of 6 August shows that sea breeze transport precursors from the metropolitan area transport to remote parts of the Kanto region and affect ozone concentrations along the penetration path. Moreover, results of the No_chem case simulations show increasing ozone concentrations without secondary formation. This increase results from entrainment of upper residual ozone through the development of the planetary boundary layer. An upper air residual ozone was contributed to by the non-metropolitan area being larger than the metropolitan area.

Two episodes shown in this paper indicate that contributions to high ozone concentration in the inland Kanto region, especially in the morning, and the contribution of non-metropolitan areas constitute the majority of high ozone generation, while the contribution of the metropolitan area was small in the calculation period. But as shown in Figs. 6 and 8, contributions of precursors emitted from the metropolitan area to ozone concentration were sometimes comparable to contributions of non-metropolitan area along the path of the sea breeze. Therefore, the results of the present study will not deny the importance of transportation of precursors emitted from metropolitan area for air quality of Kanto region.

## REFERENCES

Byun, D.W., Schere, K.L. (2006) Review of the governing equations, computational algorithms, and other components of the Model-3 Community Multiscale Air Quality (CMAQ) modeling system. Applied Mechanics Reviews 59, 51-77.

Emmons, L.K., Walters, S., Hess, P.G., Lamarque, J.-F., Pfister, G.G., Fillmore, D., Granier, C., Guenther, A., Kinnison, D., Laepple, T., Orlando, J., Tie, X., Tyndall, G., Wiedinmyer, C., Baugghcum, S.L., Kloster, S. (2010) Description and evaluation of the Model for Ozone and Related chemical Tracers, version 4 (MO ZART-4). Gescientific Model Development 3, 43-67.

Hosoi, S., Yoshikado, H., Sekiguchi, K., Wang, Q., Sakamoto, K. (2011) Daytime meteorological structures causing elevated photochemical oxidants concentrations in north Kanto, Japan. Atmospheric Environment 45, 4421-4428.

Kiriyama, Y., Hayami, H., Awasaki, T., Miura, K., Kumagai, K., Yamaguchi, N. (2012) Influence of development of mixing layer for ozone concentration in inland Kanto area in summertime. Journal of Japan Society for Atmospheric Environment 47, 81-86. (in Japanese)

Lin, C.-H., Wu, Y.-L., Lai, C.-H. (2010) Ozone reservoir layers in a coastal environment - a case study in southern Taiwan. Atmospheric Chemistry and Physics 10, 4439-4452.

Muramatsu, H. (1980) A Case Study of the Transport of the Stratospheric Ozone into the Troposphere. Papers in Meteorology and Geophysics 31, 97-105.

Niwano, M., Takigawa, M., Takahashi, M., Akimoto, H., Nakazato, M., Nagai, T., Sakai, T., Mano, Y. (2007) Evaluation of Vertical Ozone Profiles Simulated by WRF/Chem Using Lidar-Observed Data. SOLA 3, 133-136.

Pochanart, P., Akimoto, H., Kinjo, Y., Tanimoto, H. (2002) Surface ozone at four remote island sites and the preliminary assessment of the exceedances of its critical level in Japan. Atmospheric Environment 36, 4235-4250.

Schade, G.W., Khan, S., Park, C., Boedeker, I. (2011) Rural Southeast Texas Air Quality Measurements dur-

ing the 2006 Texas Air Quality Study. Journal of the Air & Waate Management Association 61, 1070-1081.

Shimadera, H., Hayami, H., Morino, Y., Ohara, T., Chatani, S., Hasegawa., S., Kaneyasu, N. (2013) Analysis of Summer-time Atmospheric Transport of Fine Particulate Matter in Northeast Asia. Asia-Pacific Journal of Atmospheric Science 49, 347-360.

Shimadera, H., Hayami, H., Ohara, T., Morino, Y., Takami, A., Irei, S. (2014) Numerical simulation of extreme air pollution by fine particulate matter in China in winter 2013. Asian Journal of Atmospheric Environment (now printing).

Skamarock, W.C., Klemp, J.B., Dudhia, J., Gill, D.O., Baker, D.M., Duda, M.G., Huang, X.-Y., Wang, W., Powers, J.G. (2008) A description of the advanced research WRF version 3. NCAR Technical Note, NCAR/TN-475+STR.

Wakamatsu, S., Ogawa, Y., Murano, K., Goi, K., Aburamoto, Y. (1983) Aircraft survey of the secondary photochemcal pollutants covering the Tokyo metropolitan area. Atmospheric Environment 17, 827-835.

(Received 17 May 2014, revised 19 November 2014, accepted 27 November 2014)